Please cite this article in press as: Wang et al., Basic enables selection-free efficient knockin of large DNA in primary human T cells, Molecular Therapy (2025), https://doi.org/10.1016/j.ymthe.2025.12.064

Molecular Therapy
Original Article

Basic enables selection-free efficient knockin of large DNA in primary human T cells

Kexin Wang,[1,6] Xiaorui Li,[1,6] Jin Li,[1,6] Zhuoying Yu,[1,2] Pan Li,[1] Yuyang Xie,[1] Jinxin Liu,[1] Honglin Huang,[1] Shanshan Zhang,[1] Mengqiao Zhang,[1] Wenju Ma,[1] Fei Gao,[1] Xuguang Du,[1] Jianxun Wang,[3,4] Mario R. Capecchi,[5] and Sen Wu[1,2]

[1]Frontiers Science Center for Molecular Design Breeding (MOE), State Key Laboratory of Animal Biotech Breeding, College of Biological Sciences, China Agricultural University, Beijing 100193, China; [2]Sanya Institute of China Agricultural University, Sanya 572024, China; [3]School of Life Sciences, Beijing University of Chinese Medicine, Beijing 102488, China; [4]Shenzhen Cell Valley Pharmaceuticals, Shenzhen 518118, China; [5]Department of Human Genetics, University of Utah School of Medicine, Salt Lake City, UT 84112, USA

Efficient and precise insertion of large DNA fragments into primary human T cells has remained a bottleneck for gene and cell therapy. We present BaEVshort-AAV6 site-specific integration for CAR T (BASIC), a modular platform that combines BaEVshort-pseudotyped virus-like particles for Cas9 RNP delivery with AAV6 donor vectors for homology-directed repair. BASIC achieves >85% knockin efficiency without drug selection or electroporation, preserving cell viability while enabling multiplex genome engineering. Edited chimeric antigen receptor (CAR)-T cells show uniform CAR expression, enhanced cytotoxicity, and complete tumor clearance *in vivo*. BASIC offers a clinically scalable solution for next-generation cell therapies.

INTRODUCTION

Precise, efficient, and safe integration of large transgenes into defined genomic loci is a longstanding goal in gene therapy and regenerative medicine. For decades, homologous-recombination-based gene targeting has been hampered by low efficiency, typically <5% even with selection markers, making it unsuitable for clinical applications.[1,2] The advent of CRISPR-Cas9 technology further enhanced homologous directed repair (HDR) efficiencies to 5%–30% in selected cell types[3–7]; however, HDR remains inefficient in primary immune cells, especially for knockin of large therapeutic constructs.

Numerous strategies have been explored to overcome the limitations of low HDR efficiency, including non-homologous end joining (NHEJ) inhibition,[8,9] HDR-promoting compounds,[10] donor template engineering,[11,12] and cell-cycle synchronization.[13] However, these approaches often show marginal benefit in primary human cells, particularly for integrating large payloads. Furthermore, these approaches often rely on electroporation or drug selection, which can cause substantial cytotoxicity and hinder scalability. As a result, no existing platform offers a broadly applicable, electroporation-free, and clinically scalable solution for efficient large-fragment integration in primary immune cells.

In parallel, chimeric antigen receptor (CAR)-T cell therapy has revolutionized hematologic cancer treatment,[14,15] but current manufacturing approaches rely on random integration of transgenes via retroviruses or lentiviruses, raising concerns about insertional mutagenesis and transgene silencing.[16–19] While site-specific CAR knockin via CRISPR-Cas9 has attracted intense interest for its potential to improve product uniformity and safety,[20–22] current strategies remain technically demanding and inefficient, often requiring electroporation of Cas9 ribonucleoprotein complexes (RNPs) together with adeno-associated virus (AAV) or double-stranded DNA donors. All of these available multi-step processes suffer from high cell loss and batch-to-batch variability, posing major hurdles for clinical translation and large-scale manufacturing.

Virus-like particles (VLPs) retain the natural cell-entry capacity of viruses but lack a genome, eliminating integration risk while serving as efficient carriers for Cas9 RNPs or mRNAs.[23,24] Although VLP-based approaches have been explored for T cell genome editing, an effective strategy for generating CAR-T cells with high-efficiency, site-specific integration has yet to be established.[25,26]

Here we introduce BaEVshort-AAV6 site-specific integration for CAR T (BASIC)—a clinically scalable genome-editing platform that integrates two potent viral systems: (1) BaEVshort-pseudotyped virus-like particles to deliver Cas9 RNPs efficiently into primary

Received 15 August 2025; accepted 22 December 2025;
https://doi.org/10.1016/j.ymthe.2025.12.064.

[6]These authors contributed equally

Correspondence: Xuguang Du, Frontiers Science Center for Molecular Design Breeding (MOE), State Key Laboratory of Animal Biotech Breeding, College of Biological Sciences, China Agricultural University, Beijing 100193, China.
E-mail: xuguangdu@cau.edu.cn
Correspondence: Jianxun Wang, School of Life Sciences, Beijing University of Chinese Medicine, Beijing 102488, China.
E-mail: jianxun.wang@bucm.edu.cn
Correspondence: Mario R. Capecchi, Department of Human Genetics, University of Utah School of Medicine, Salt Lake City, UT 84112, USA.
E-mail: mario.capecchi@genetics.utah.edu
Correspondence: Sen Wu, Frontiers Science Center for Molecular Design Breeding (MOE), State Key Laboratory of Animal Biotech Breeding, College of Biological Sciences, China Agricultural University, Beijing 100193, China.
E-mail: swu@cau.edu.cn

Please cite this article in press as: Wang et al., Basic enables selection-free efficient knockin of large DNA in primary human T cells, Molecular Therapy (2025), https://doi.org/10.1016/j.ymthe.2025.12.064

T cells, and (2) AAV6 vectors encoding CAR donor templates flanked by homology arms. BASIC eliminates the need for electroporation, drug selection, or random integration and consistently achieves >85% knockin and >95% knockout efficiencies in human primary T cells.

BASIC-engineered CAR-T cells exhibit enhanced antitumor activity, cytokine secretion, and long-term persistence *in vitro* and *in vivo*, surpassing conventional lentiviral-based methods. Moreover, BASIC supports multiplex editing and application in natural killer (NK) cells, offering a generalizable, modular framework for building next-generation cellular immunotherapies.

RESULTS

VLPs enable site-specific integration by delivering CRISPR-Cas9

Previous studies have demonstrated that VLPs can efficiently deliver a variety of genome-editing cargos into mammalian cells.[25,27–31] In parallel, lentiviral vectors have been engineered into non-integrating forms (NILVs) through mutations in the integrase recognition sites,[32,33] allowing them to serve as transient donor templates for homology-directed repair (Figures S1A and S1B). To test this strategy, we first co-delivered VLPs[30] loaded with Cas9 RNPs and an NILV-based donor designed to correct a point mutation in the BFP gene into HEK293T cells stably expressing BFP from the AAVS1 locus (Figures S1C and S1D). This approach achieved approximately 26% GFP conversion (Figure S1E), indicating successful HDR-mediated correction.

We next extended this approach to large-fragment integration. An NILV donor encoding a CD19-specific CAR (3.3 kb) flanked by TRAC-specific homology arms was co-delivered with VLPs into Jurkat cells (Figure S1F). In the presence of the DNA-PKcs inhibitor M3814, we observed 34.7% CAR^+ cells (Figure S1G), demonstrating that NILV donors can support integration of therapeutic-sized cargo.

However, when the same system was applied to primary human T cells, knockin efficiency dropped sharply to ∼3.2% (Figures S1H and S1I). Given that VSV-G-pseudotyped lentiviral vectors can efficiently transduce activated T cells, this reduction is unlikely to be explained by impaired viral entry alone. Rather, our results point to two intrinsic bottlenecks in this configuration: first, VSV-G-pseudotyped VLPs may not efficiently support Cas9 RNP delivery and genome editing in primary T cells; second, NILV-derived HDR donors cannot be dose-escalated to the high template copy numbers achievable with AAV vectors. Together, these limitations substantially constrain the amount of genome-editing machinery available per cell, resulting in the modest KI efficiency observed.

BaEVshort-pseudotyped VLPs outperform VSV-G for Cas9 delivery in primary T cells

To improve VLP transduction efficiency in T cells, we replaced the conventional VSV-G envelope with the baboon endogenous virus (BaEV) envelope, which utilizes ASCT1/2 receptors highly expressed on activated T cells.[34–36] A previously reported BaEV envelope mutant further enhances T cell transduction but induces pronounced syncytium formation in packaging cells.[37] To address this, we engineered a truncated envelope (BaEVshort) lacking the C-terminal R peptide (Figure 1A). BaEVshort-pseudotyped VLPs achieved a 6-fold increase in capsid protein (p30) levels compared to VSV-G-VLPs, indicating improved packaging efficiency (Figure 1B). Notably, all BaEV envelope variants tested similarly produced significantly higher physical titers than VSV-G, with no detectable differences observed among the BaEV variants themselves.

To prevent envelope-mediated fusion during production,[38] we generated ASCT1/2 double-knockout HEK293T packaging cells (Figures S2A and S2B). BaEVshort-VLPs produced from ASCT1/2 double-knockout HEK293T cells were directly applied to human primary T cells for transduction (Figure 1C). VSV-G-VLPs were generated using wild-type HEK293T cells under otherwise identical conditions. Both VLP types shared identical internal components, differing only in their envelope glycoproteins (Figure S2C). We next compared VLPs pseudotyped with different BaEV variants to VSV-G VLPs under matched conditions. BaEVshort-pseudotyped VLPs yielded the highest editing efficiency in primary T cells, whereas BaEVRless showed the lowest efficiency (Figure 1D). These results indicate that BaEVshort is the most effective BaEV-derived envelope for genome editing in T cells, while BaEVRless—despite its advantages for lentiviral vector production[37]—is suboptimal for retrovirus-based VLP delivery. Furthermore, modifying the single guide RNA (sgRNA) scaffold to enhance Cas9-RNP complex stability[29] boosted editing efficiencies by 1.5- to 2.5-fold across multiple targets (Figure 1E).

Importantly, BaEVshort-VLPs did not impair T cell proliferation (Figure S2D). Flow cytometry analysis demonstrated that TRAC-targeting VLP transduction resulted in ∼96% CD3 knockout in both $CD4^+$ and $CD8^+$ T cell subsets without selection (Figure S2E). Titration of BaEVshort plasmid input revealed that, while physical titers declined at higher doses, editing efficiency improved (Figures 1F and S2F), likely due to increased envelope density per particle.

BaEVshort-enveloped MLV VLPs enable multiplex gene editing in T and NK cells

NK cell-based immunotherapies are gaining clinical momentum due to their low risk of graft-versus-host disease and cytokine release syndrome.[39,40] However, genetic modification of primary NK cells remains challenging due to poor transduction efficiency with conventional envelopes such as VSV-G. Given the high expression of ASCT1/2 on NK cells,[41] we hypothesized that BaEVshort-VLPs may offer superior editing performance. Indeed, when BaEVshort-VLPs were used to transduce primary NK cells, editing efficiencies exceeded 80% at TRAC and B2M loci, and they surpassed 60% at programmed cell death protein 1(PD-1) and CTLA4—significantly higher than those achieved with VSV-G-VLPs (Figure S3A).

Please cite this article in press as: Wang et al., Basic enables selection-free efficient knockin of large DNA in primary human T cells, Molecular Therapy (2025), https://doi.org/10.1016/j.ymthe.2025.12.064

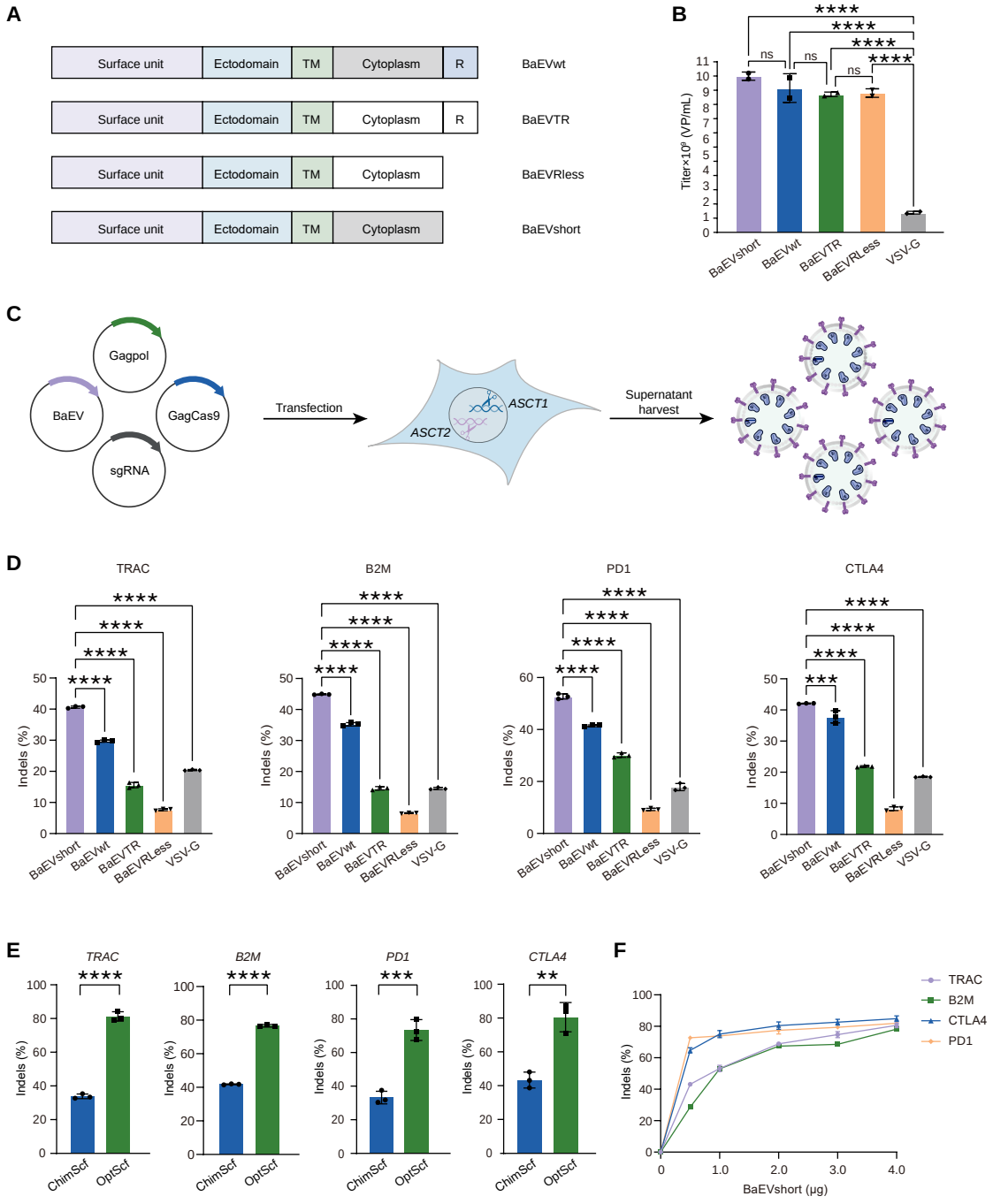

Figure 1. MLV VLPs with BaEVshort envelope enhance gene editing efficiency in T cells

(A) Structural schematics of BaEVwt, BaEVTR, BaEVRless, and BaEVshort envelope variants. (B) Physical titers of VLPs pseudotyped with BaEVwt, BaEVTR, BaEVRless, BaEVshort, or VSV-G, measured by p30 ELISA ($n = 2$ technical replicates). (C) Schematic of BaEV-VLP production and T cell transduction. Created with BioRender.com. (D) Gene editing efficiency at four genomic loci (TRAC, PD-1, B2M, CTLA4) in T cells transduced with VLPs pseudotyped with VSV-G or BaEV variants. (E) Optimized sgRNA scaffold improves Cas9-mediated editing via BaEVshort-VLPs across multiple targets. (F) Effect of BaEVshort envelope plasmid titration on editing efficiency at TRAC, PD-1, B2M, and CTLA4. Data are presented as the mean ± SD from triplicates ($n = 3$ independent healthy donors). p values were calculated by one-way ANOVA with Tukey's multiple-comparisons test (B), Dunnett's multiple-comparisons test (D), and unpaired t tests: $^{**}p < 0.01$, $^{***}p < 0.001$, and $^{****}p < 0.0001$; ns, not significant.

Please cite this article in press as: Wang et al., Basic enables selection-free efficient knockin of large DNA in primary human T cells, Molecular Therapy (2025), https://doi.org/10.1016/j.ymthe.2025.12.064

To support the development of off-the-shelf CAR-T therapies, multiplex gene editing is required to ablate immunogenicity (TRAC, B2M) and enhance persistence (PD-1, CTLA4).[42,43] We generated multiplexed VLPs by co-packaging multiple sgRNAs and tested their performance in both T and NK cells. In primary T cells, dual and triple editing efficiencies reached 62%–78% and 52%–61%, respectively. NK cells also supported double editing at 61%–67% and triple editing at 23%–31% (Figures S3B-E). Notably, these high multiplexing efficiencies were achieved without viral concentration or Retronectin pre-coating.[37] These findings demonstrate that BaEVshort-pseudotyped VLPs support robust, high-efficiency multiplex genome editing in both T and NK cells, providing a versatile and scalable platform for the generation of universal immune effector cells.

BaEVshort-VLPs paired with AAV6 donor enable one-step gene knockout and targeted CAR knockin

Since lentiviral vectors require reverse transcription in target cells before providing an HDR template, we opted to use AAV as the CAR donor, whose single-stranded DNA genome can efficiently serve as a template for HDR in T cells.[44,45] To streamline CAR-T cell engineering, we combined BaEVshort-VLPs for Cas9 RNP delivery with an AAV6 donor encoding a CD19 CAR flanked by TRAC-specific homology arms and matched sgRNA cut sites (Figures 2A and 2B). This configuration enables simultaneous T cell receptor (TCR) knockout and CAR knockin in a single transduction step, constituting the basis of our BASIC platform.

Across a range of AAV6 multiplicities of infection (MOIs), we observed robust CAR^+ cell generation, with efficiencies increasing from 38.5% at low MOIs to over 85% at an MOI of 2×10^5 (Figure 2C). CAR expression was uniform across $CD4^+$ and $CD8^+$ subsets (Figure 2D), and >94% TRAC knockout was observed. CAR expression was restricted to $CD3^-$ cells, indicating high targeting fidelity (Figures 2E and S4A). Off-target analysis via next-generation sequencing (NGS) showed no detectable indels at predicted loci (Figure S4B), and junction PCR with Sanger sequencing confirmed precise integration (Figure S4C). To assess the impact of AAV dose on CAR-T cell performance, we evaluated viability, proliferation, and phenotype across different AAV MOIs. On days 4 and 10 post infection, CAR-T cells generated with MOIs of 2×10^4 to 4×10^5 all maintained high viability (>90%), with no significant differences among groups (Figure 2F). Proliferation after tumor cell stimulation increased with higher CAR-positive rates, consistent with enhanced CAR-mediated activation (Figure 2G). Under antigen stimulation, TIM3 expression gradually increased with higher AAV MOI, likely reflecting the greater proportion of CAR-positive cells rather than a direct effect of AAV itself. Importantly, at the optimal MOI of 2×10^5, TIM3 levels in BASIC-edited cells remained lower than those in retrovirally generated CAR-T cells, indicating that early exhaustion was largely mitigated (Figure 2H).

We further validated this approach at the *PD1* locus, achieving up to 75.2% CAR^+ cells with similarly high precision (Figures S5A–S5E). These results establish the BASIC system as a flexible, high-fidelity platform for programmable CAR integration at multiple therapeutic loci.

Multiplex gene knockout and knockin enable potent allogeneic CAR-T cells

To produce hypoimmunogenic, allogeneic CAR-T cells, we simultaneously disrupted TRAC and B2M while inserting a CD19 CAR into the TRAC locus. Under optimized conditions, double-knockout efficiencies exceeded 55%–58% in both $CD4^+$ and $CD8^+$ cells, and CAR^+ rates exceeded 80% (Figures 3A and 3B). Across six donors, we observed consistent outcomes: >95% CD3 knockout, ∼80% CAR positivity, and ∼50% double knockout (Figure 3C).

Compared to retroviral (RV) methods, BASIC CAR-T cells exhibited more uniform CAR expression (Figures 3D and 3E and 3F). No significant difference in CAR positivity was observed among $CD3^-$ T cells between the BASIC CAR-T cells and control groups (Figure 3G). These features highlight improved manufacturing consistency and support the scalability of the platform.

To further evaluate whether BASIC can accommodate a broader range of knockout and knockin combinations, we designed additional donors targeting the B2M and CTLA4 loci. These achieved CAR positivity rates of 80.4% and 56.8%, respectively (Figure S6A). We then assessed the feasibility of generating fully universal CAR-T cells by combining multi-gene knockouts with site-specific CAR integration (Figure S6B). When using B2M-targeting BASIC together with PD-1, TRAC, or CTLA4 knockouts, knockin efficiencies remained between 72% and 80%. For CTLA4-targeting BASIC, efficiencies ranged from 52% to 67%, whereas TRAC-targeting BASIC maintained 79%–82% CAR insertion (Figures S6C, S6D and S6E). As expected, knockin efficiencies varied by genomic locus.

Importantly, robust and consistent knockout efficiencies were maintained across all editing combinations, demonstrating the scalability and versatility of BASIC for generating next-generation universal CAR-T cell products.

BASIC CAR-T cells exhibit superior cytotoxicity and persistence *in vitro*

To evaluate the antitumor activity of CAR-T cells generated via the BASIC, we performed *in vitro* cytotoxicity assays using CD19-expressing Nalm6 lymphoma cells engineered to co-express GFP and luciferase (Nalm6-GFP-Luc). BASIC CAR-T cells showed greater cytolytic activity than RV controls across a range of effector:target (E:T) ratios, as measured by luciferase signal (Figures 4A and S7A). To evaluate target cell death induced by CAR-T cells, Annexin V staining was performed after 12-h co-culture at the indicated E:T ratios. Early apoptosis of target cells was assessed by Annexin V staining and flow cytometry. BASIC CAR-T cells induced higher levels of apoptosis compared with the RV CAR-T group (Figures 4B and S7B). Real-time IncuCyte imaging confirmed earlier and more durable tumor killing (Figures 4C and S7C).

Please cite this article in press as: Wang et al., Basic enables selection-free efficient knockin of large DNA in primary human T cells, Molecular Therapy (2025), https://doi.org/10.1016/j.ymthe.2025.12.064

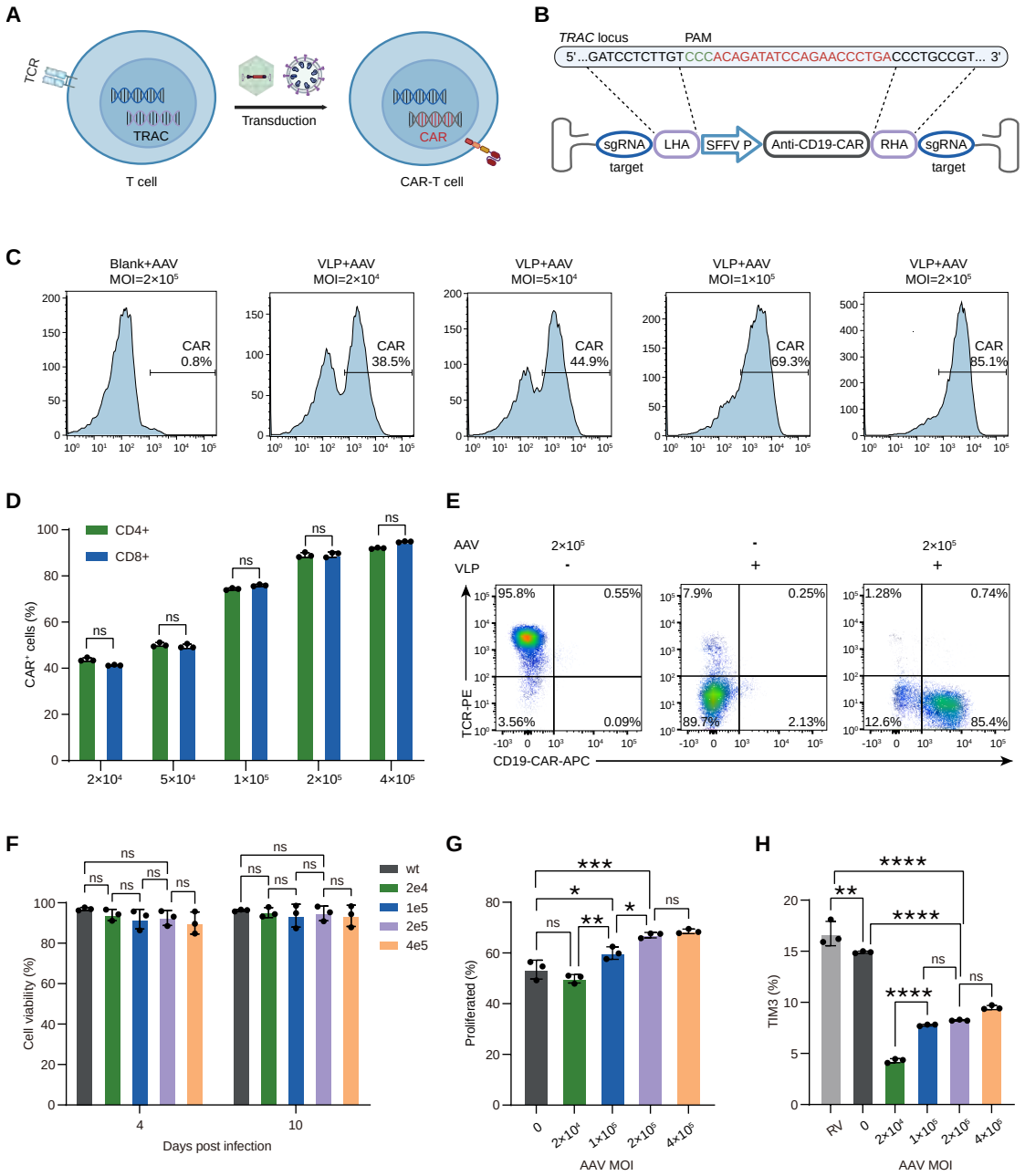

Figure 2. One-step gene knockout and CD19 CAR knockin via BASIC

(A) Simultaneous TRAC knockout and CAR knockin achieved through a one-step infection with AAV6 donor and VLP-delivered RNP. Created with BioRender.com. (B) Structure of AAV6 donor construct containing SFFV-driven CD19 CAR flanked by TRAC homology arms. (C) CAR expression in T cells following co-transduction with BaEVshort-VLPs and AAV6 at indicated MOIs. (D) CAR positivity in $CD4^+$ and $CD8^+$ T cells across different AAV doses. (E) *TRAC* knockout and co-expression of CAR in $CD3^-$ T cells assessed by flow cytometry. Representative flow cytometry plots are shown for one donor. (F) Viability of CAR-T cells on days 4 and 10 post infection, assessed by flow cytometry using Zombie NIR dye. (G) Proliferation of CAR-T cells following tumor cell stimulation, assessed using CellTrace Violet. (H) TIM3 expression on CAR-T cells after tumor cell stimulation, measured by flow cytometry. Data are presented as the mean ± SD from triplicates ($n = 3$ independent healthy donors). p values were calculated by Sidak's multiple-comparisons test (D and F) and Tukey's multiple-comparisons test (G and H): $^*p < 0.05$, $^{**}p < 0.01$, $^{***}p < 0.001$, and $^{****}p < 0.0001$; ns, not significant.

In serial challenge assays, BASIC CAR-T cells maintained cytotoxic function over three rounds of tumor stimulation, while RV CAR-T cells displayed functional exhaustion (Figures 4D and S7D). BASIC CAR-Ts also demonstrated enhanced proliferation (Figures 4E and S7E) and secreted higher levels of interleukin (IL)-2, tumor necrosis factor (TNF)-α, interferon (IFN)-γ, and granzyme B upon target

Please cite this article in press as: Wang et al., Basic enables selection-free efficient knockin of large DNA in primary human T cells, Molecular Therapy (2025), https://doi.org/10.1016/j.ymthe.2025.12.064

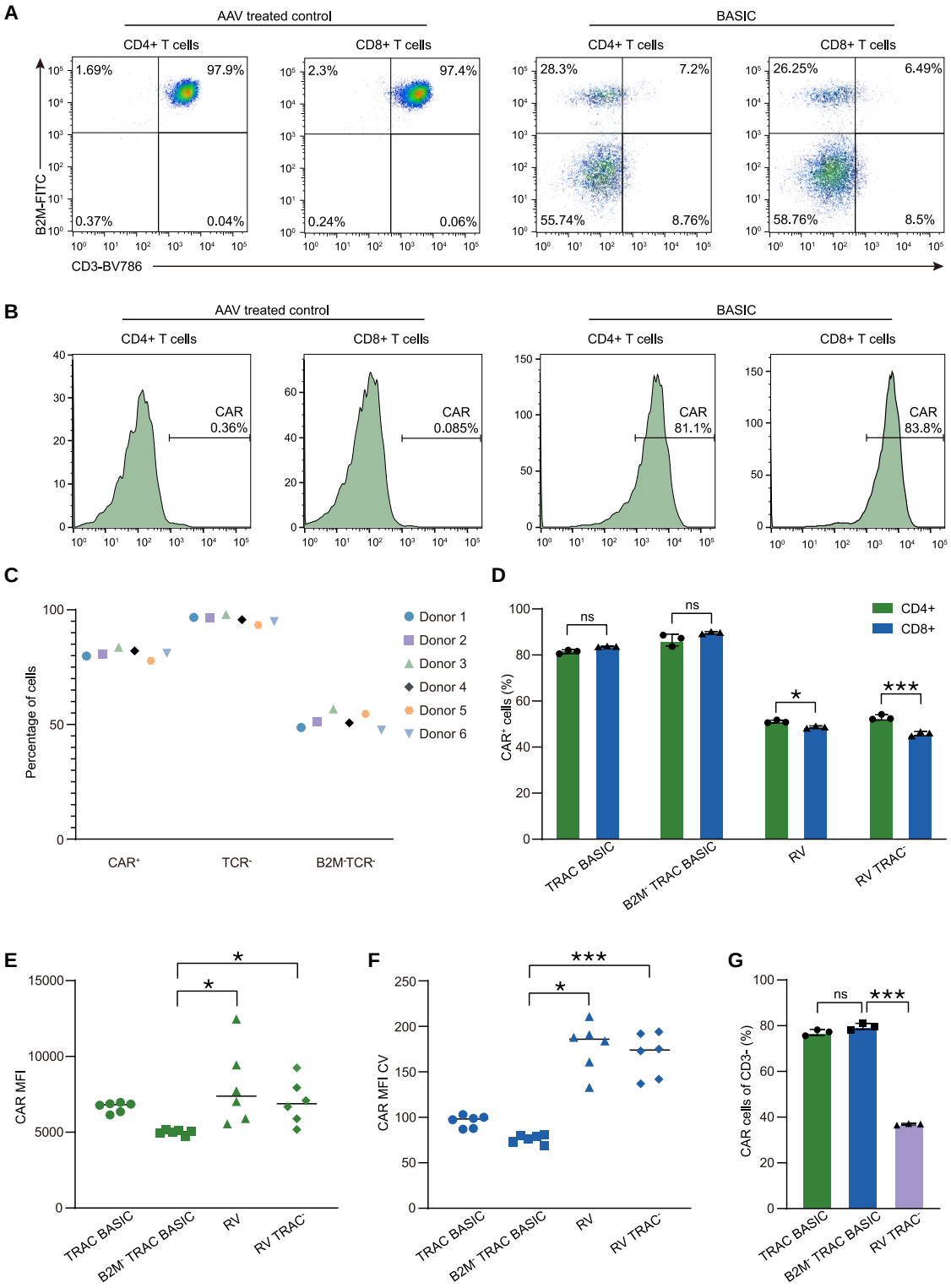

Figure 3. Simultaneous TRAC/B2M knockout and TRAC-targeted CD19 CAR knockin in primary T cells

(A) Dual knockout efficiency (TRAC, B2M) in CD4$^+$ and CD8$^+$ T cells after co-transduction with BaEVshort-VLPs and AAV6. Surface expression of B2M and TCR was analyzed by flow cytometry on day 5 post transduction. (B) CAR expression in double-knockout T cell subsets. (C) CAR$^+$ rates and knockout efficiency across six donors. (D) CAR expression in CD4$^+$ and CD8$^+$ T cells comparing BASIC, retroviral (RV), and RV TCR$^-$ groups. (E–F) CAR expression uniformity shown by median fluorescence intensity

(legend continued on next page)

Please cite this article in press as: Wang et al., Basic enables selection-free efficient knockin of large DNA in primary human T cells, Molecular Therapy (2025), https://doi.org/10.1016/j.ymthe.2025.12.064

stimulation (Figures 4F and S7F). CAR-T cell survival after tumor co-culture was highest in the BASIC group (Figure S7G), reflecting their superior proliferative and cytotoxic potential.

To explore mechanisms underlying their improved function, we profiled activation and exhaustion markers. BASIC CAR-T cells upregulated CD69 and CD25 following tumor exposure (Figures 5A and 5B) while maintaining markedly lower expression of PD-1 and TIM-3 compared to RV CAR-T cells, even after repeated stimulation (Figures 5C and 5D). This phenotype is consistent with previous reports that TRAC-targeted CAR-T cells exhibit reduced early PD-1 induction due to the loss of endogenous TCR signaling,[21] which normally drives transcription of exhaustion-associated genes. In the absence of a functional TRAC complex, PD-1 expression remains low during initial antigen encounters because CAR-mediated activation does not strongly engage the same transcriptional programs as TCR signaling. However, with repeated rounds of tumor stimulation, residual CAR-driven activation and cumulative antigen exposure can eventually induce modest PD-1 upregulation, albeit to a substantially lower extent than in cells harboring randomly integrated CARs, which are more prone to tonic signaling. Together, these findings provide a mechanistic basis for the enhanced resilience of BASIC CAR-T cells to exhaustion and support their superior functional durability.

To assess whether the enhanced cytotoxicity of BASIC CAR-T cells is inherent to the delivery strategy, we generated CAR-T cells using BASIC targeted to the AAVS1 safe-harbor locus. Across increasing AAV MOIs, CAR positivity reached up to 50.3%, following a trend consistent with previously tested loci (Figures S8A). Compared with retrovirally transduced CAR-T cells under matched conditions, no significant differences were observed (Figures S8B). Notably, when comparing AAVS1 with functional loci including TRAC, PD-1, B2M, and CTLA4, TRAC-targeted CAR-T cells exhibited the highest tumor-killing activity (Figures S8C). These findings indicate that the cytotoxic potential of BASIC CAR-T cells is locus dependent, and precise integration into functional genomic sites maximizes effector function.

BASIC CAR-T cells mediate robust and durable tumor clearance *in vivo*

To evaluate the antitumor efficacy of BASIC *in vivo*, we conducted experiments as outlined (Figure 6A). Bioluminescence imaging revealed that compared with the mock-treated or untreated T cell groups, tumor cells were effectively eliminated in the BASIC, RV, and RV TCR$^-$ groups (Figure 6B).

Mice treated with BASIC CAR-T cells exhibited significantly higher levels of human IFN-γ in the blood than those in the RV and RV TCR$^-$ groups, indicating robust T cell activation shortly after treatment (Figure 6C). Furthermore, CD19 antigen was nearly undetectable in the blood, liver, spleen, and bone marrow of the BASIC group, with tumor cell residues significantly lower than in the RV and RV TCR$^-$ groups (Figure 6D). Survival analysis revealed 100% survival in the BASIC group vs. 37.5% and 62.5% in RV and RV TCR$^-$ groups, respectively (Figure 6E). Flow cytometry analysis confirmed efficient TCR disruption in the RV TCR$^-$ group, with approximately 80% loss of CD3 expression (Figures S9A and S9B). Interestingly, despite exhibiting CAR expression levels comparable to the RV CAR-T group (Figure S9C), RV TCR$^-$ cells demonstrated improved tumor control and prolonged survival *in vivo*, likely reflecting reduced tonic signaling from the endogenous TCR, which limits premature activation and supports CAR-T persistence.

Notably, TRAC-targeted BASIC CAR-T cells achieved stronger and more durable antitumor activity, reflecting both higher CAR positivity and precise site-specific integration beyond TCR deletion, thereby establishing the potent antitumor efficacy of our platform.

DISCUSSION

BASIC represents a significant advance in genome engineering for human immune cells by addressing key challenges associated with large-fragment knockin: efficiency, precision, safety, and scalability. Its core innovation lies in the combination of two clinically viable components—BaEVshort-pseudotyped VLPs and AAV6 vectors—that together enable high-efficiency, site-specific integration in primary T cells without compromising viability or requiring drug-based selection. This system eliminates the need for electroporation, enhances safety by avoiding random viral integration, and simplifies manufacturing via a one-step viral transduction protocol.

Compared to electroporation-based delivery of plasmids or RNPs—which often compromise cell viability[46,47]—our BaEVshort VLP-based approach maintains high editing efficiency while preserving cell health. We achieve >90% gene knockout and >85% targeted CAR integration at the *TRAC* locus without selection. Importantly, this platform is also applicable to NK cells, enabling over 60% editing at multiple loci, which supports the development of universal, allogeneic cell therapies.

AAV has been extensively validated in both preclinical studies and clinical trials as an efficient and safe vector for delivering donor DNA templates.[48] While multiple strategies combine AAV donors with Cas9 RNP delivery,[9,20,21,49] electroporation prior to AAV transduction increases manufacturing complexity and limits *in vivo* applicability. In contrast, VSV-G-pseudotyped lentiviral vectors efficiently deliver genes into activated T cells, but their utility as HDR donors is constrained by the limited number of donor molecules delivered per cell. Because NILV doses cannot be escalated without compromising T cell viability, reverse-transcribed donor DNA

(MFI) and coefficient of variation (CV). $n = 6$ independent healthy donors. (G) CAR$^+$ rates of CD3$^-$ T cell subsets. Data are presented as the mean ± SD from triplicates ($n \geq 3$ independent healthy donors). p values were calculated by two-way ANOVA with Tukey's multiple-comparisons test (D) and ordinary one-way ANOVA with Tukey's multiple-comparisons test (E–G): $^*p < 0.05$, $^{***}p < 0.001$; ns, not significant.

Please cite this article in press as: Wang et al., Basic enables selection-free efficient knockin of large DNA in primary human T cells, Molecular Therapy (2025), https://doi.org/10.1016/j.ymthe.2025.12.064

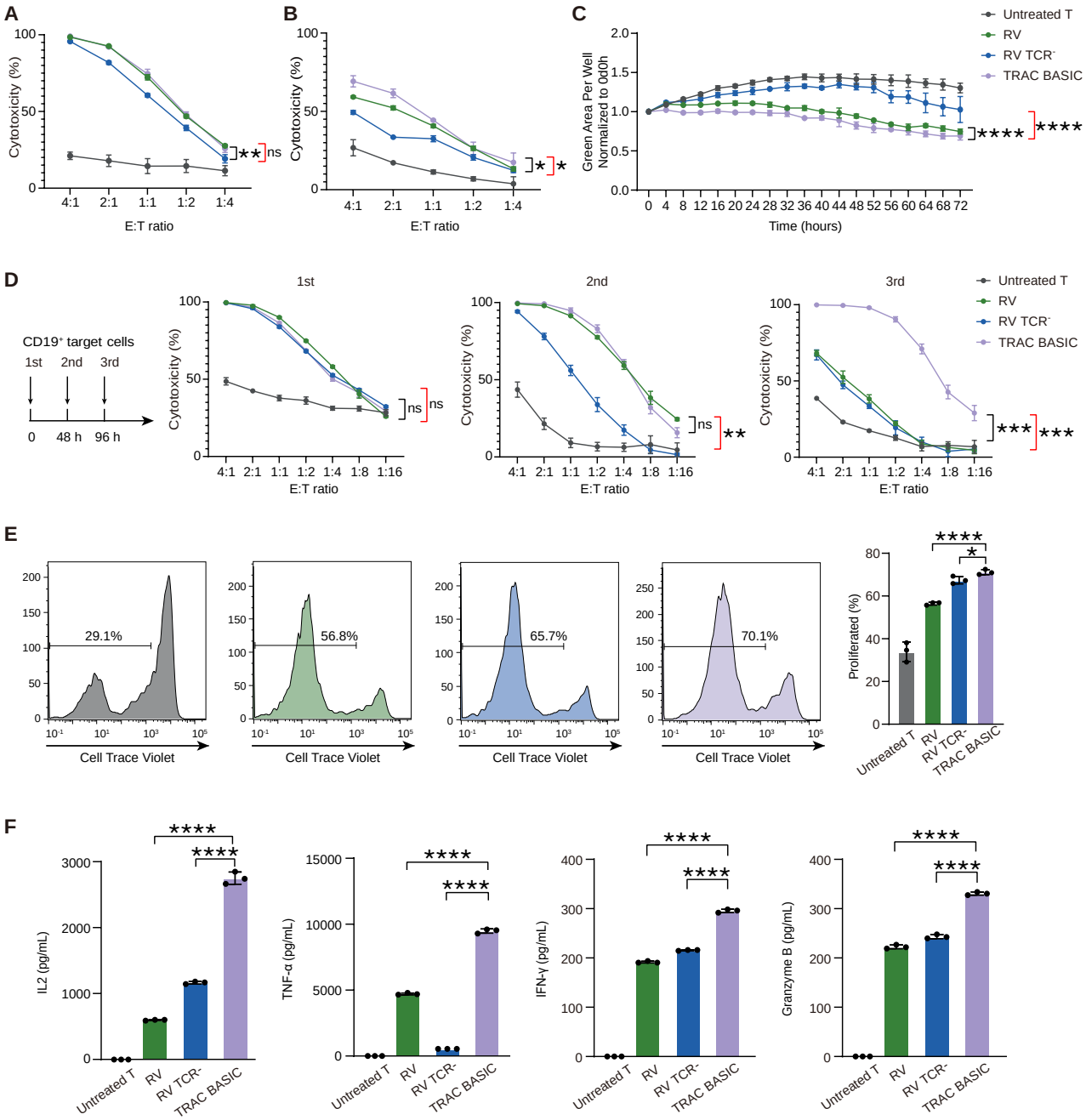

Figure 4. TRAC-BASIC CAR-T cells show superior antitumor and proliferation capacity *in vitro* compared to traditional CAR-T cells

(A) Cytotoxicity of CAR-T cells against CD19⁺ Nalm6-GFP-Luc cells measured via bioluminescence after 12-h co-culture at varying effector:target (E:T) ratios. (B) Early apoptosis of Nalm6-GFP-Luc target cells after 12-h co-culture with CAR-T cells, assessed by Annexin V staining. (C) Real-time killing kinetics of CAR-T cells over 72 h monitored using IncuCyte GFP imaging at 4-h intervals. (D) Serial tumor challenge assay measuring CAR-T durability across three rounds of stimulation. (E) T cell proliferation assessed via CellTrace Violet dilution following 48-h co-culture with Raji cells. (F) Cytokine secretion (IL-2, IFN-γ, TNF-α, granzyme B) quantified post co-culture with tumor targets. *p* values were calculated by two-way ANOVA with Tukey's multiple-comparisons test (A–D) and one-way ANOVA with Tukey's multiple-comparisons test (E and F): $^{*}p < 0.05$, $^{**}p < 0.01$, $^{***}p < 0.001$, and $^{****}p < 0.0001$. Data are presented as the mean ± SD ($n = 3$ biological replicates from independent donors). Black significance represents comparisons between BASIC and RV-treated groups, while red represents comparisons between experimental and RV KO groups (A–D).

Please cite this article in press as: Wang et al., Basic enables selection-free efficient knockin of large DNA in primary human T cells, Molecular Therapy (2025), https://doi.org/10.1016/j.ymthe.2025.12.064

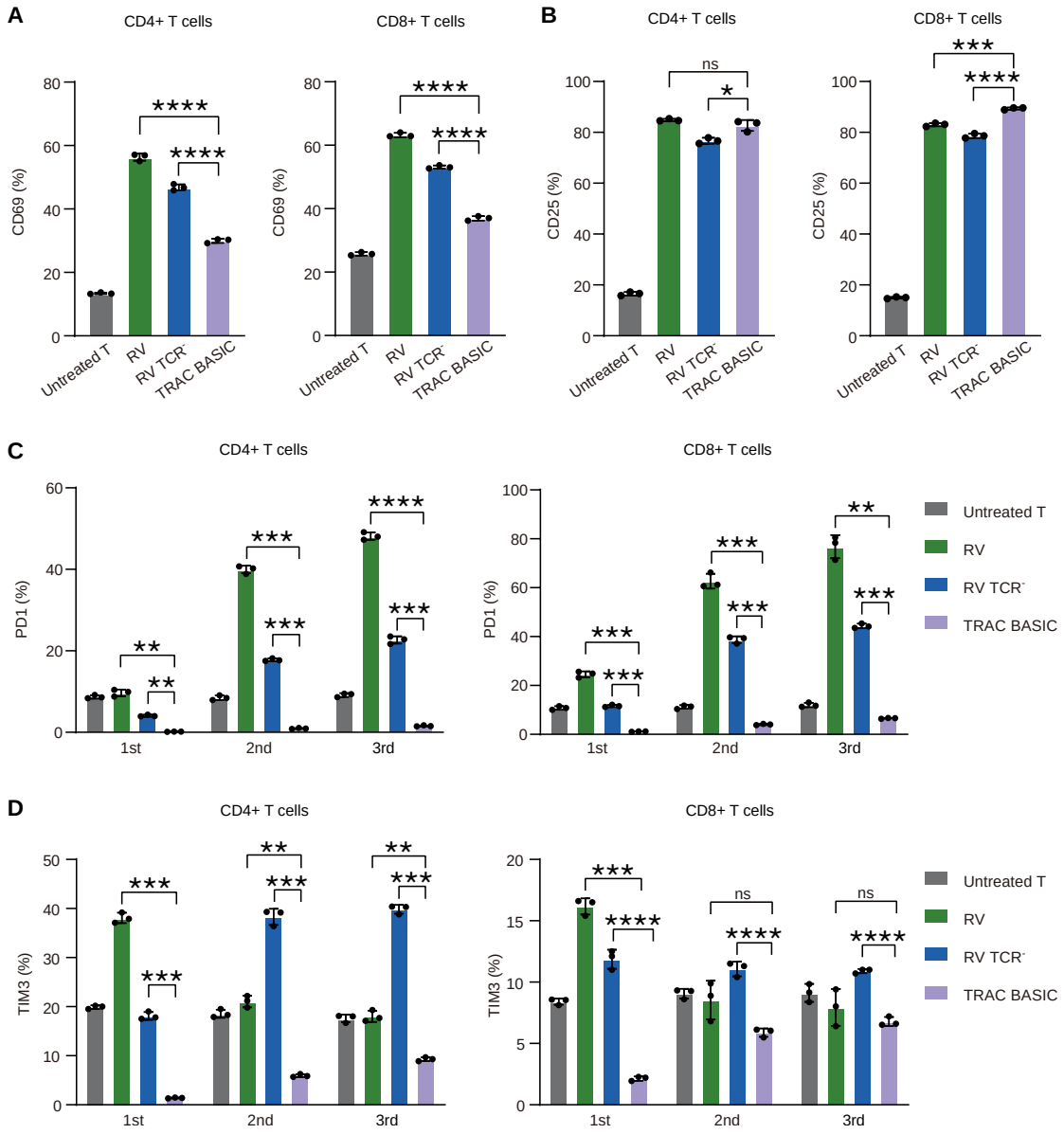

Figure 5. Phenotypic profiling of TRAC-BASIC CAR-T cells reveals enhanced activation and reduced exhaustion

(A and B) CD69 and CD25 expression following 24-h co-culture with tumor cells in $CD4^+$ and $CD8^+$ CAR-T subsets. (C and D) PD-1 and TIM3 expression levels following first, second, and third tumor stimulations in CAR-T cells generated by BASIC or RV methods. *p* values were calculated by one-way ANOVA with Tukey's multiple-comparisons test (A and B) and two-way ANOVA with Tukey's multiple-comparisons test (C and D): $^*p < 0.05$, $^{**}p < 0.01$, $^{***}p < 0.001$, and $^{****}p < 0.0001$. Data are presented as the mean ± SD ($n = 3$ biological replicates from independent donors). Ns, not significant.

remains low, forming a bottleneck for HDR. Indeed, recent studies of lentivirus-derived nanoparticles indicate that IDLV-derived templates are present at modest levels,[50] and our observation that AAV-mediated knockin efficiency drops sharply when MOI is reduced further supports the conclusion that HDR efficiency in primary T cells is strongly dependent on donor template abundance. By pairing BaEVshort-VLPs with AAV6 donors, BASIC enables precise genome editing with abundant template availability and a single-step viral transduction workflow, overcoming the cytotoxicity and complexity associated with traditional electroporation-based methods.

VLPs have been established as safe and efficient delivery vehicles, with demonstrated success in gene therapy applications.[28,30,31,51] Compared to earlier VLP-based CAR-T approaches that relied on lentiviral or RV vectors for random CAR integration,[25,52]

Please cite this article in press as: Wang et al., Basic enables selection-free efficient knockin of large DNA in primary human T cells, Molecular Therapy (2025), https://doi.org/10.1016/j.ymthe.2025.12.064

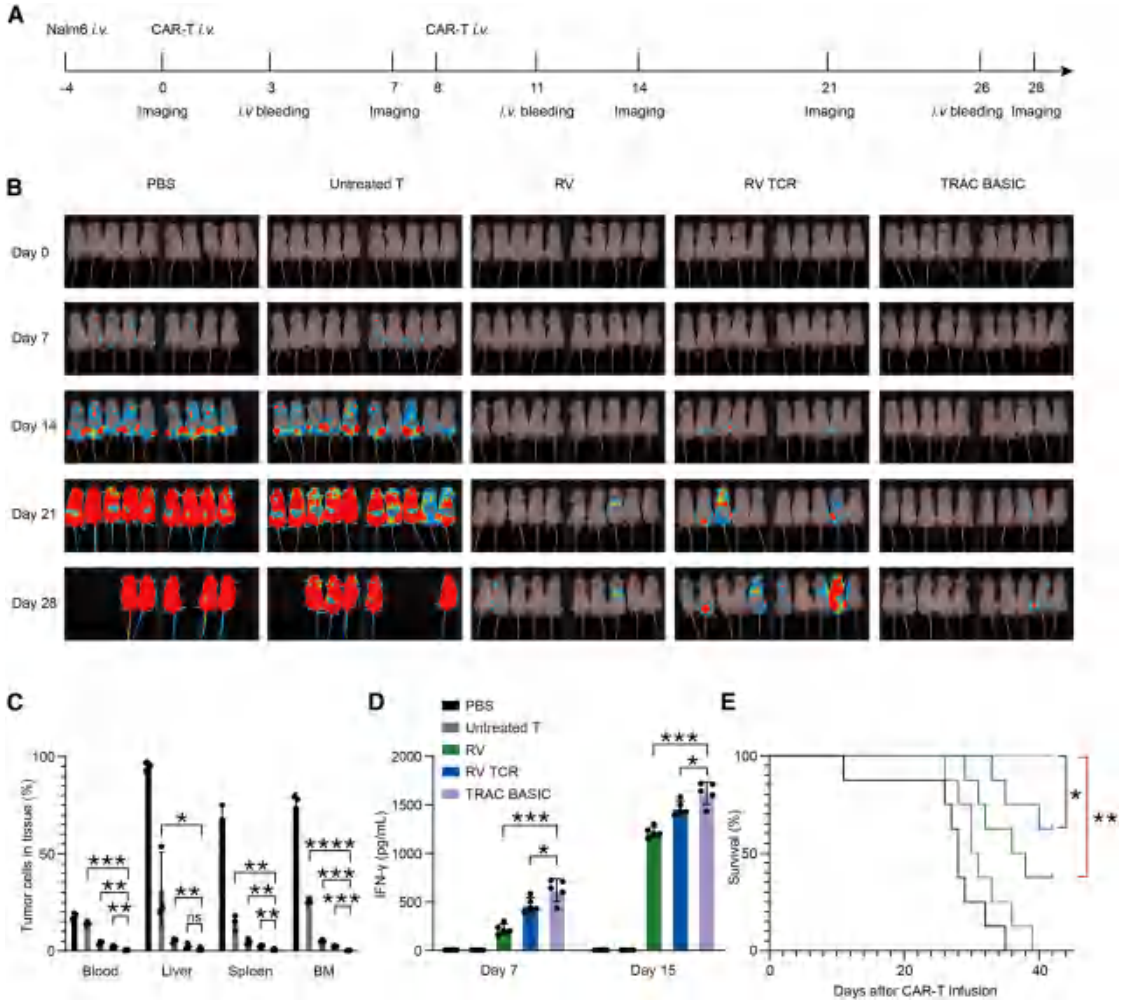

Figure 6. TRAC-BASIC CAR-T cells exhibit potent antitumor activity *in vivo*

(A) Experimental timeline for xenograft model using Nalm6-GFP-Luc cells in immunodeficient mice. For each group, 10 mice were monitored for survival, while five mice were allocated for terminal tissue harvest to assess tumor burden in blood, liver, spleen, and bone marrow. (B) Bioluminescence imaging of tumor cell growth following different treatments on the indicated days after CAR-T cell infusion. $n = 10$ mice per group. (C) $CD19^+$ tumor cell burden in blood, liver, spleen, and bone marrow on day 28. $n = 3$ mice per group. (D) Serum IFN-γ levels measured on day 3 post infusion. $n = 5$ mice per group. (E) Kaplan-Meier survival curves over 42 days. Mice were euthanized by cervical dislocation. $n = 10$ mice per group. p values were calculated by two-way ANOVA with Tukey's multiple-comparisons test (C), one-way ANOVA with Tukey's multiple-comparisons test (D), and the Mantel-Cox log rank test (E). $^*p < 0.05$, $^{**}p < 0.01$, $^{***}p < 0.001$, and $^{****}p < 0.0001$. Data are presented as the mean ± SD.

BASIC employs VLPs solely for transient Cas9 RNP delivery and uses AAV for high-fidelity homology-directed repair. Furthermore, by flanking AAV donors with matched sgRNA cut sites,[53] we reduce concatemer insertions and enhance knockin precision. This strategy improves both the efficacy and safety of engineered cells.

The BASIC platform is designed to maximize efficiency while minimizing production costs in CAR-T cell engineering. By achieving high KO/KI and CAR-T positivity rates in primary T cells, BASIC requires substantially fewer starting cells and smaller-scale *ex vivo* culture, thereby reducing vector consumption per patient. Moreover, its compatibility with allogeneic, "off-the-shelf" CAR-T manufacturing further decreases vector usage and shortens production timelines. To lower production costs, we are also developing stable packaging cell lines expressing murine leukemia virus (MLV) gagpol, Gag-Cas9, and BaEVshort envelope, a strategy known to improve batch-to-batch consistency and reduce reliance on repeated transient transfection. At the industry level, continuous improvements in viral-vector manufacturing—such as high-density fixed-bed bioreactors, plasmid-free helper systems, and continuous downstream purification—are rapidly driving down per-dose AAV costs.[54,55] Because BASIC relies on modular AAV and VLP components that align with these maturing platforms, its production workflow can be

readily standardized and scaled within existing GMP infrastructures. Together, these features support the economic feasibility and industrial scalability of BASIC for future clinical translation.

Recent studies have shown that envelope selection critically affects the efficiency and tropism of RV and lentiviral vectors. Replacing the VSV-G envelope of lentiviral vectors with heterologous viral glycoproteins—such as those from measles virus, baboon endogenous retrovirus, Cocal virus, Nipah virus, or Sendai virus—can substantially improve transduction of hematopoietic stem cells, B cells, T cells, and NK cells.[56] In addition, codon-optimized gibbon ape leukemia virus (GALV) envelopes have been shown to increase lentiviral titers and enhance T cell transduction.[57] Further approaches involve antibody-coupled envelope proteins to specifically enhance the transduction of targeted cell types, such as T cells and NK cells, thereby improving the *in vivo* applicability of viral vectors.[58–60] In this study, our BASIC platform utilizes BaEVshort-pseudotyped VLPs to enhance delivery efficiency into primary human T cells, enabling high-efficiency multiplexed KO/KI and integration of large transgenes such as CARs. Future iterations may incorporate base or prime editors, allowing precise, double-strand-break-free genome modification and further enhancing therapeutic safety.[51,61] Moreover, with appropriate envelope optimization, BASIC may support *in vivo* delivery applications[62]—extending its utility beyond *ex vivo* cell manufacturing.

In conclusion, BASIC offers a robust, safe, and scalable system for precise large-fragment genome integration. It enables researchers and clinicians to overcome longstanding barriers in cell therapy development and provides a generalizable solution for next-generation gene and cell engineering applications.

MATERIALS AND METHODS

Cell culture

HEK293T cells were maintained in Dulbecco's modified Eagle's medium (DMEM, Gibco) supplemented with 10% fetal bovine serum (FBS, Gibco), 1 mM sodium pyruvate (Gibco), 1× non-essential amino acids (NEAAs, Gibco), and 1% penicillin-streptomycin (Gibco). Cells were cultured at 37°C in a 5% CO_2 incubator. Nalm-6-GFP-Luc and Raji cells were grown in RPMI-1640 medium (Gibco) with10% FBS and 1% penicillin-streptomycin. Stable cell lines expressing GFP and firefly luciferase (ffLuc) were generated by lentiviral transduction and validated by fluorescence and bioluminescence assays. All cell lines were confirmed to be mycoplasma-free by periodic PCR-based testing.

Isolation and culture of human primary T cells and NK cells

Human peripheral blood mononuclear cells (PBMCs) were obtained from human peripheral blood provided by Shanghai Liquan Hospital and the hPBMC isolation service provided by Milecell Biotechnologies. T cells cultured in X-VIVO 15 medium (Lonza) supplemented with 10% FBS (Gibco), recombinant human IL-2 (100 U/mL, PeproTech), and T cell TransAct (Miltenyi Biotec). NK cell cultivation was conducted with a commercial-grade culture medium (YOCON Biotech). Cells were activated for 3 days prior to transduction and maintained at 37°C in 5% CO_2.

Plasmid construction

Plasmids used for VLP production and gene editing were generated using standard molecular cloning. The VSV-G envelope plasmid (pCMV-VSV-G), MLV gagpol (pBS-CMV-gagpol), and MLV gag-Cas9 (pMLV-Gag-Cas9) were obtained from Addgene. The BaEV envelope sequence and its truncated variant (BaEVRless and BaEVshort) were synthesized (General Biology) and cloned under a CAG promoter. sgRNAs were cloned into expression vectors via BbsI restriction sites. HDR donor constructs were generated by inserting SFFV-driven CD19-CAR between homology arms into a pAAV-MCS (multiple cloning sites) vector. Recombinant AAV6 was packaged using triple transfection and purified by Guangzhou PackGene Biotechnology. All constructs were verified by sequencing.

VLP production and titration

To produce BaEV- or VSV-G-pseudotyped VLPs, HEK293T or ASCT1/2-knockout HEK293T cells were seeded in 10-cm dishes at 5×10^6 cells per plate and incubated for 24 h prior to transfection. Transfection was performed using jetPRIME (Polyplus) with plasmids encoding MLV gagpol, gagCas9, sgRNA, and envelope (BaEV or VSV-G), in a 3.375:1.125:4.4:3-μg ratio unless otherwise indicated. For multiplex editing, multiple sgRNA plasmids were co-transfected in a 2.2:2.2-μg ratio. Supernatants were harvested at 48 h post transfection, clarified by 400 × *g* centrifugation, and filtered through a 0.45-μm polyvinylidene fluoride (PVDF) membrane. VLPs were stored at −80°C until use. Physical titers were quantified by ELISA using anti-p30 antibodies (GenScript) according to the manufacturer's protocol.

T and NK cell transduction

Activated T cells were transduced with BaEV-VLPs at 8×10^9 particles per reaction in the presence of 8 μg/mL Polybrene (Sigma) and 2 μM M3814 (Selleck). For gene knockin, AAV6 was added at indicated MOIs simultaneously with VLPs. Transductions were performed in 12-well plates by centrifugation at 2,000 rpm for 60 min at 30°C. The same protocol was applied to NK cell transduction. Cells were harvested 48–72 h post transduction for downstream analyses.

Genomic DNA extraction and editing analysis

Genomic DNA was extracted using the DNeasy Blood & Tissue Kit (Qiagen). On-target and off-target editing were quantified by targeted PCR amplification and deep sequencing. Libraries were prepared using NEBNext Ultra II DNA Library Prep Kit (NEB), and sequencing was performed on an Illumina MiSeq. CRISPResso2 was used for indel analysis. Off-target sites were predicted using Cas-OFFinder, and editing was quantified as the proportion of reads with insertions or deletions. Sanger sequencing was used to validate HDR integration at homology arms.

Flow cytometry analysis

T cells were stained in PBS with 2% FBS using antibodies against human CD3 (APC/PE/BV786), β2M (FITC), PD-1 (PE), CD4 (BV785),

CD69 (PerCP), CD25 (PE), TIM-3 (PE Cy7), and CAR (anti-cMyc, Alexa Fluor 647; all from BioLegend) and CD8 (BUV395, from BD). Flow cytometric analysis was performed on a BD FACSAria Fusion Flow Cytometer (BD Biosciences), and data were analyzed using FlowJo v10.8 (BD Biosciences). For analysis of gene editing, knockout efficiency was calculated by comparing the frequency of positive cells in edited samples to the frequency of negative cells in untransduced controls.

Bioluminescence imaging-based cytolysis assay

To evaluate the CAR-T cell-mediated tumor cell lysis capacity, CAR-T cells or untransduced T cells (untreated T) were co-cultured with CD19-expressing Nalm6-GFP-Luc cells at varying E:T ratios for 12 h. Luminescence signals reflecting luciferase activity were quantified using a SpectraMax i3x multimode microplate reader (Molecular Devices). Cytolytic activity was calculated using the formula: cytolysis (%) = [1 − (experimental lysis − spontaneous lysis)/(maximum lysis − spontaneous lysis)] × 100%, where maximum lysis was determined by detergent-mediated cell disruption, and spontaneous lysis represented baseline signal from target cells alone. All experiments were performed in triplicate.

Fluorescence-based kinetic analysis via IncuCyte

Untreated T cells were co-cultures with Nalm6-GFP-Luc cells at a 1:1 E:T ratio. Real-time kinetic monitoring was conducted using the IncuCyte S3 Live-Cell Analysis System (Sartorius). Phase-contrast and GFP fluorescence images were acquired every 4 h for 72 h. Total GFP intensity per well, normalized to initial values, served as a quantitative metric for viable GFP^+ tumor cells.

Flow-cytometry-based cytolysis assessment

CAR-T or untreated T cells were co-cultured with Nalm6-GFP-Luc cells at defined E:T ratios for 12 h. Apoptotic tumor cells were identified by APC-Annexin V staining (BioLegend). Samples were analyzed on a BD FACSAria Fusion cytometer with data processed using FlowJo v10.8.1. Apoptotic rate was calculated as the percentage of GFP^+/Annexin V^+ cells relative to total cells. Triplicate experiments were conducted.

Cytokine release profiling

Supernatants from CAR-T/tumor cell co-cultures (12-h incubation) were analyzed using the LEGENDple Human Cytokine Panel (13-plex, BioLegend) following manufacturer protocols. Bead arrays were acquired via flow cytometry, with cytokine concentrations interpolated from standard curves.

CAR-T cell proliferation assay

CAR-T and untreated T cells were labeled with CellTrace Violet (Thermo Fisher) per manufacturer guidelines. Labeled cells were co-cultured with $CD19^+$ Raji cells (1:1 E:T ratio) for 48 h. Proliferation kinetics were quantified by flow cytometric analysis of dye dilution (BD FACSAria Fusion, FlowJo v10.8.1). Three independent experiments were performed.

Xenograft tumor model in immunodeficient mice

Female NPG/Vst mice (NOD-PrkdcscidIl2rgnull, 6–8 weeks old) under specific-pathogen-free conditions were purchased from Vitalstart (Beijing, China). Mice received intravenous inoculation of 2×10^5 Nalm6-GFP-Luc cells via tail vein. Four days post engraftment, tumor-bearing mice were randomized into five groups (n = 15/group): PBS, untreated T, RV, RV TCR−, and TRAC KO/KI. For each group, a total of 15 mice were used, of which 10 were allocated for survival monitoring and five were predetermined for terminal tissue harvest to assess tumor burden in blood, liver, spleen, and bone marrow. CAR-T cells (2×10^6 cells/mouse) were administered intravenously on day 0 and day 8. Tumor burden was monitored weekly using the Fusion FX7 Spectra imaging system (Vilber Lourmat) following luciferin injection.

Peripheral blood was collected via retro-orbital puncture at day 3 post treatment for IFN-γ quantification (Human IFN-γ EILSA Kit, R&D Systems). At day 26, $CD19^+$ cell persistence was assessed by APC-conjugated CD19 staining (flow cytometry). Terminal tissue harvest (liver, spleen, bone marrow) was performed at day 31 post tumor inoculation. Human CD19 expression in blood and tissues was analyzed via flow cytometry (BD FACSAria Fusion, FlowJo v10.8.1). The study duration was 42 days.

Institutional review board statement

PBMCs were obtained from human peripheral blood provided by Shanghai Liquan Hospital (scheme number: Z-ZJMS—21-10-001) and hPBMC isolation service provided by Milecell Biotechnologies. Animal experiments were approved by the Animal Welfare Committee of China Agricultural University (approval no. AW03111202-3-1).

Statistics

Experimental data are presented as the mean ± SD as described in the figure legends. Data were analyzed by unpaired t test, one-way ANOVA, two-way ANOVA, or Mantel-Cox log rank test as indicated using GraphPad software. $p < 0.05$ was considered statistically significant. Asterisks are used to indicate significance: $^{****}p < 0.0001$, $^{***}p < 0.001$, $^{**}p < 0.01$, $^{*}p < 0.05$; NS, not significant.

DATA AND CODE AVAILABILITY

- The authors confirm that the data supporting the findings of this study are available within the article and its supplemental information or available from the corresponding authors upon reasonable request.

ACKNOWLEDGMENTS

We are grateful for continuous support from the Wu lab members. This work was supported by the National Key Research and Development Program of China (grant nos. 2021YFA0805901, 2023YFC3402004, 2023YFC3404301, and 2023YFF0724700), the Biological Breeding-National Science and Technology Major Project (grant no. 2024ZD04077), Agricultural Science and Technology Major Project, the Innovative Project of State Key Laboratory of Animal Biotech Breeding (grant no. 2024SKLAB 1-8), the Chinese Universities Scientific Fund (grant no. 2024TC167), and the 2115 Talent Development Program of China Agricultural University.

AUTHOR CONTRIBUTIONS

K.W., X.L., J. Li, and S.W. designed the study. K.W., X.L., J. Li, J. Liu, S.Z., H.H., and Y.X. performed the experiments. K.W., X.L., J. Li, Z.Y., P.L., M.Z., W.M., F.G., X.D., J.W., M. R.C., and S.W. analyzed the data. K.W., X.L., J. Li, S.W., and M.R.C. wrote the manuscript with input from all authors. X.D., J.W., M.R.C., and S.W. supervised the study. All authors approved the manuscript for submission and publication.

DECLARATION OF INTERESTS

Patent applications related to this research have been submitted.

SUPPLEMENTAL INFORMATION

Supplemental information can be found online at https://doi.org/10.1016/j.ymthe.2025.12.064.

REFERENCES

1. Thomas, K.R., Folger, K.R., and Capecchi, M.R. (1986). High frequency targeting of genes to specific sites in the mammalian genome. Cell *44*, 419–428. https://doi.org/10.1016/0092-8674(86)90463-0.
2. Thomas, K.R., and Capecchi, M.R. (1987). Site-directed mutagenesis by gene targeting in mouse embryo-derived stem cells. Cell *51*, 503–512. https://doi.org/10.1016/0092-8674(87)90646-5.
3. Hsu, P.D., Lander, E.S., and Zhang, F. (2014). Development and Applications of CRISPR-Cas9 for Genome Engineering. Cell *157*, 1262–1278. https://doi.org/10.1016/j.cell.2014.05.010.
4. Ran, F.A., Hsu, P.D., Wright, J., Agarwala, V., Scott, D.A., and Zhang, F. (2013). Genome engineering using the CRISPR-Cas9 system. Nat. Protoc. *8*, 2281–2308. https://doi.org/10.1038/nprot.2013.143.
5. Chu, V.T., Weber, T., Wefers, B., Wurst, W., Sander, S., Rajewsky, K., and Kühn, R. (2015). Increasing the efficiency of homology-directed repair for CRISPR-Cas9-induced precise gene editing in mammalian cells. Nat. Biotechnol. *33*, 543–548. https://doi.org/10.1038/nbt.3198.
6. Maruyama, T., Dougan, S.K., Truttmann, M.C., Bilate, A.M., Ingram, J.R., and Ploegh, H.L. (2015). Increasing the efficiency of precise genome editing with CRISPR-Cas9 by inhibition of nonhomologous end joining. Nat. Biotechnol. *33*, 538–542. https://doi.org/10.1038/nbt.3190.
7. He, X., Tan, C., Wang, F., Wang, Y., Zhou, R., Cui, D., You, W., Zhao, H., Ren, J., and Feng, B. (2016). Knock-in of large reporter genes in human cells via CRISPR/Cas9-induced homology-dependent and independent DNA repair. Nucleic Acids Res. *44*, e85. https://doi.org/10.1093/nar/gkw064.
8. Fu, Y.-W., Dai, X.-Y., Wang, W.-T., Yang, Z.-X., Zhao, J.-J., Zhang, J.-P., Wen, W., Zhang, F., Oberg, K.C., Zhang, L., et al. (2021). Dynamics and competition of CRISPR–Cas9 ribonucleoproteins and AAV donor-mediated NHEJ, MMEJ and HDR editing. Nucleic Acids Res. *49*, 969–985. https://doi.org/10.1093/nar/gkaa1251.
9. Selvaraj, S., Feist, W.N., Viel, S., Vaidyanathan, S., Dudek, A.M., Gastou, M., Rockwood, S.J., Ekman, F.K., Oseghale, A.R., Xu, L., et al. (2024). High-efficiency transgene integration by homology-directed repair in human primary cells using DNA-PKcs inhibition. Nat. Biotechnol. *42*, 731–744. https://doi.org/10.1038/s41587-023-01888-4.
10. Song, J., Yang, D., Xu, J., Zhu, T., Chen, Y.E., and Zhang, J. (2016). RS-1 enhances CRISPR/Cas9- and TALEN-mediated knock-in efficiency. Nat. Commun. *7*, 10548. https://doi.org/10.1038/ncomms10548.
11. Nguyen, D.N., Roth, T.L., Li, P.J., Chen, P.A., Apathy, R., Mamedov, M.R., Vo, L.T., Tobin, V.R., Goodman, D., Shifrut, E., et al. (2020). Polymer-stabilized Cas9 nanoparticles and modified repair templates increase genome editing efficiency. Nat. Biotechnol. *38*, 44–49. https://doi.org/10.1038/s41587-019-0325-6.
12. Shy, B.R., Vykunta, V.S., Ha, A., Talbot, A., Roth, T.L., Nguyen, D.N., Pfeifer, W.G., Chen, Y.Y., Blaeschke, F., Shifrut, E., et al. (2023). High-yield genome engineering in primary cells using a hybrid ssDNA repair template and small-molecule cocktails. Nat. Biotechnol. *41*, 521–531. https://doi.org/10.1038/s41587-022-01418-8.
13. Webber, B.R., Johnson, M.J., Skeate, J.G., Slipek, N.J., Lahr, W.S., DeFeo, A.P., Mills, L.J., Qiu, X., Rathmann, B., Diers, M.D., et al. (2024). Cas9-induced targeted integration of large DNA payloads in primary human T cells via homology-mediated end-joining DNA repair. Nat. Biomed. Eng. *8*, 1553–1570. https://doi.org/10.1038/s41551-023-01157-4.
14. June, C.H., and Sadelain, M. (2018). Chimeric Antigen Receptor Therapy. N. Engl. J. Med. *379*, 64–73. https://doi.org/10.1056/NEJMra1706169.
15. Schuster, S.J., Bishop, M.R., Tam, C.S., Waller, E.K., Borchmann, P., McGuirk, J.P., Jäger, U., Jaglowski, S., Andreadis, C., Westin, J.R., et al. (2019). Tisagenlecleucel in Adult Relapsed or Refractory Diffuse Large B-Cell Lymphoma. N. Engl. J. Med. *380*, 45–56. https://doi.org/10.1056/NEJMoa1804980.
16. Michieletto, D., Lusic, M., Marenduzzo, D., and Orlandini, E. (2019). Physical principles of retroviral integration in the human genome. Nat. Commun. *10*, 575. https://doi.org/10.1038/s41467-019-08333-8.
17. Bulcha, J.T., Wang, Y., Ma, H., Tai, P.W.L., and Gao, G. (2021). Viral vector platforms within the gene therapy landscape. Sig Transduct Target Ther. *6*, 53. https://doi.org/10.1038/s41392-021-00487-6.
18. Perica, K., Jain, N., Scordo, M., Patel, R., Eren, O.C., Patel, U., Gundem, G., Domenico, D., Mitra, S., Socci, N.D., et al. (2025). CD4+ T-Cell Lymphoma Harboring a Chimeric Antigen Receptor Integration in TP53. N. Engl. J. Med. *392*, 577–583. https://doi.org/10.1056/NEJMoa2411507.
19. Ellis, J. (2005). Silencing and Variegation of Gammaretrovirus and Lentivirus Vectors. Hum. Gene Ther. *16*, 1241–1246. https://doi.org/10.1089/hum.2005.16.1241.
20. Dai, X., Park, J.J., Du, Y., Kim, H.R., Wang, G., Errami, Y., and Chen, S. (2019). One-step generation of modular CAR-T cells with AAV–Cpf1. Nat. Methods *16*, 247–254. https://doi.org/10.1038/s41592-019-0329-7.
21. Eyquem, J., Mansilla-Soto, J., Giavridis, T., van der Stegen, S.J.C., Hamieh, M., Cunanan, K.M., Odak, A., Gönen, M., and Sadelain, M. (2017). Targeting a CAR to the TRAC locus with CRISPR/Cas9 enhances tumour rejection. Nature *543*, 113–117. https://doi.org/10.1038/nature21405.
22. Zhang, J., Hu, Y., Yang, J., Li, W., Zhang, M., Wang, Q., Zhang, L., Wei, G., Tian, Y., Zhao, K., et al. (2022). Non-viral, specifically targeted CAR-T cells achieve high safety and efficacy in B-NHL. Nature *609*, 369–374. https://doi.org/10.1038/s41586-022-05140-y.
23. Choi, J.G., Dang, Y., Abraham, S., Ma, H., Zhang, J., Guo, H., Cai, Y., Mikkelsen, J.G., Wu, H., Shankar, P., and Manjunath, N. (2016). Lentivirus pre-packed with Cas9 protein for safer gene editing. Gene Ther. *23*, 627–633. https://doi.org/10.1038/gt.2016.27.
24. Prel, A., Caval, V., Gayon, R., Ravassard, P., Duthoit, C., Payen, E., Maouche-Chretien, L., Creneguy, A., Nguyen, T.H., Martin, N., et al. (2015). Highly efficient *in vitro* and *in vivo* delivery of functional RNAs using new versatile MS2-chimeric retrovirus-like particles. Mol. Ther. Methods Clin. Dev. *2*, 15039. https://doi.org/10.1038/mtm.2015.39.
25. Hamilton, J.R., Tsuchida, C.A., Nguyen, D.N., Shy, B.R., McGarrigle, E.R., Sandoval Espinoza, C.R., Carr, D., Blaeschke, F., Marson, A., and Doudna, J.A. (2021). Targeted delivery of CRISPR-Cas9 and transgenes enables complex immune cell engineering. Cell Rep. *35*, 109207. https://doi.org/10.1016/j.celrep.2021.109207.
26. Gutierrez-Guerrero, A., Abrey Recalde, M.J., Mangeot, P.E., Costa, C., Bernadin, O., Périan, S., Fusil, F., Froment, G., Martinez-Turtos, A., Krug, A., et al. (2021). Baboon Envelope Pseudotyped "Nanoblades" Carrying Cas9/gRNA Complexes Allow Efficient Genome Editing in Human T, B, and CD34+ Cells and Knock-in of AAV6-Encoded Donor DNA in CD34+ Cells. Front Genome Ed *3*, 604371. https://doi.org/10.3389/fgeed.2021.604371.
27. Lyu, P., Wang, L., and Lu, B. (2020). Virus-Like Particle Mediated CRISPR/Cas9 Delivery for Efficient and Safe Genome Editing. Life *10*, 366. https://doi.org/10.3390/life10120366.
28. Ling, S., Yang, S., Hu, X., Yin, D., Dai, Y., Qian, X., Wang, D., Pan, X., Hong, J., Sun, X., et al. (2021). Lentiviral delivery of co-packaged Cas9 mRNA and a Vegfa-targeting guide RNA prevents wet age-related macular degeneration in mice. Nat. Biomed. Eng. *5*, 144–156. https://doi.org/10.1038/s41551-020-00656-y.
29. Haldrup, J., Andersen, S., Labial, A.R.L., Wolff, J.H., Frandsen, F.P., Skov, T.W., Rovsing, A.B., Nielsen, I., Jakobsen, T.S., Askou, A.L., et al. (2023). Engineered lentivirus-derived nanoparticles (LVNPs) for delivery of CRISPR/Cas ribonucleoprotein

complexes supporting base editing, prime editing and in vivo gene modification. Nucleic Acids Res. *51*, 10059–10074. https://doi.org/10.1093/nar/gkad676.

30. Banskota, S., Raguram, A., Suh, S., Du, S.W., Davis, J.R., Choi, E.H., Wang, X., Nielsen, S.C., Newby, G.A., Randolph, P.B., et al. (2022). Engineered virus-like particles for efficient *in vivo* delivery of therapeutic proteins. Cell *185*, 250–265.e16. https://doi.org/10.1016/j.cell.2021.12.021.

31. Ling, S., Zhang, X., Dai, Y., Jiang, Z., Zhou, X., Lu, S., Qian, X., Liu, J., Selfjord, N., Satir, T.M., et al. (2025). Customizable virus-like particles deliver CRISPR–Cas9 ribonucleoprotein for effective ocular neovascular and Huntington's disease gene therapy. Nat. Nanotechnol. *20*, 543–553. https://doi.org/10.1038/s41565-024-01851-7.

32. Shaw, A., and Cornetta, K. (2014). Design and Potential of Non-Integrating Lentiviral Vectors. Biomedicines *2*, 14–35. https://doi.org/10.3390/biomedicines2010014.

33. Nightingale, S.J., Hollis, R.P., Pepper, K.A., Petersen, D., Yu, X.-J., Yang, C., Bahner, I., and Kohn, D.B. (2006). Transient Gene Expression by Nonintegrating Lentiviral Vectors. Mol. Ther. *13*, 1121–1132. https://doi.org/10.1016/j.ymthe.2006.01.008.

34. Bernadin, O., Amirache, F., Girard-Gagnepain, A., Moirangthem, R.D., Lévy, C., Ma, K., Costa, C., Nègre, D., Reimann, C., Fenard, D., et al. (2019). Baboon envelope LVs efficiently transduced human adult, fetal, and progenitor T cells and corrected SCID-X1 T-cell deficiency. Blood Adv. *3*, 461–475. https://doi.org/10.1182/bloodadvances.2018027508.

35. Gutierrez-Guerrero, A., Abrey Recalde, M.J., Mangeot, P.E., Costa, C., Bernadin, O., Périan, S., Fusil, F., Froment, G., Martinez-Turtos, A., Krug, A., et al. (2021). Baboon Envelope Pseudotyped "Nanoblades" Carrying Cas9/gRNA Complexes Allow Efficient Genome Editing in Human T, B, and CD34+ Cells and Knock-in of AAV6-Encoded Donor DNA in CD34+ Cells. Front. Genome Ed. *3*, 604371. https://doi.org/10.3389/fgeed.2021.604371.

36. Levy, C., Fusil, F., Amirache, F., Costa, C., Girard-Gagnepain, A., Negre, D., Bernadin, O., Garaulet, G., Rodriguez, A., Nair, N., et al. (2016). Baboon envelope pseudotyped lentiviral vectors efficiently transduce human B cells and allow active factor IX B cell secretion *in vivo* in NOD/SCIDγc-/- mice. J. Thromb. Haemost. *14*, 2478–2492. https://doi.org/10.1111/jth.13520.

37. Girard-Gagnepain, A., Amirache, F., Costa, C., Lévy, C., Frecha, C., Fusil, F., Nègre, D., Lavillette, D., Cosset, F.-L., and Verhoeyen, E. (2014). Baboon envelope pseudotyped LVs outperform VSV-G-LVs for gene transfer into early-cytokine-stimulated and resting HSCs. Blood *124*, 1221–1231. https://doi.org/10.1182/blood-2014-02-558163.

38. Klatt, D., Sereni, L., Liu, B., Genovese, P., Schambach, A., Verhoeyen, E., Williams, D.A., and Brendel, C. (2024). Engineered packaging cell line for the enhanced production of baboon-enveloped retroviral vectors. Mol. Ther. Nucleic Acids *35*, 102389. https://doi.org/10.1016/j.omtn.2024.102389.

39. Marin, D., Li, Y., Basar, R., Rafei, H., Daher, M., Dou, J., Mohanty, V., Dede, M., Nieto, Y., Uprety, N., et al. (2024). Safety, efficacy and determinants of response of allogeneic CD19-specific CAR-NK cells in CD19+ B cell tumors: a phase 1/2 trial. Nat. Med. *30*, 772–784. https://doi.org/10.1038/s41591-023-02785-8.

40. Hosseinalizadeh, H., Wang, L.-S., Mirzaei, H., Amoozgar, Z., Tian, L., and Yu, J. (2025). Emerging combined CAR-NK cell therapies in cancer treatment: Finding a dancing partner. Mol. Ther. *33*, 2406–2425. https://doi.org/10.1016/j.ymthe.2024.12.057.

41. Colamartino, A.B.L., Lemieux, W., Bifsha, P., Nicoletti, S., Chakravarti, N., Sanz, J., Roméro, H., Selleri, S., Béland, K., Guiot, M., et al. (2019). Efficient and Robust NK-Cell Transduction With Baboon Envelope Pseudotyped Lentivector. Front. Immunol. *10*, 2873. https://doi.org/10.3389/fimmu.2019.02873.

42. Dagher, O.K., and Posey, A.D. (2023). Forks in the road for CAR T and CAR NK cell cancer therapies. Nat. Immunol. *24*, 1994–2007. https://doi.org/10.1038/s41590-023-01659-y.

43. Depil, S., Duchateau, P., Grupp, S.A., Mufti, G., and Poirot, L. (2020). 'Off-the-shelf' allogeneic CAR T cells: development and challenges. Nat. Rev. Drug Discov. *19*, 185–199. https://doi.org/10.1038/s41573-019-0051-2.

44. Nyberg, W.A., Ark, J., To, A., Clouden, S., Reeder, G., Muldoon, J.J., Chung, J.-Y., Xie, W.H., Allain, V., Steinhart, Z., et al. (2023). An evolved AAV variant enables efficient genetic engineering of murine T cells. Cell *186*, 446–460.e19. https://doi.org/10.1016/j.cell.2022.12.022.

45. Westhaus, A., Barba-Sarasua, E., Chen, Y., Hsu, K., Scott, S., Knight, M., Haase, F., Mesa Mora, S., Houghton, B.C., Roca-Pinilla, R., et al. (2025). Tailoring capsid-directed evolution technology for improved AAV-mediated CAR-T generation. Mol. Ther. *33*, 2801–2818. https://doi.org/10.1016/j.ymthe.2024.12.012.

46. Kebriaei, P., Singh, H., Huls, M.H., Figliola, M.J., Bassett, R., Olivares, S., Jena, B., Dawson, M.J., Kumaresan, P.R., Su, S., et al. (2016). Phase I trials using *Sleeping Beauty* to generate CD19-specific CAR T cells. J. Clin. Invest. *126*, 3363–3376. https://doi.org/10.1172/JCI86721.

47. An, J., Zhang, C.-P., Qiu, H.-Y., Zhang, H.-X., Chen, Q.-B., Zhang, Y.-M., Lei, X.-L., Zhang, C.-X., Yin, H., and Zhang, Y. (2024). Enhancement of the viability of T cells electroporated with DNA via osmotic dampening of the DNA-sensing cGAS–STING pathway. Nat. Biomed. Eng. *8*, 149–164. https://doi.org/10.1038/s41551-023-01073-7.

48. Kuzmin, D.A., Shutova, M.V., Johnston, N.R., Smith, O.P., Fedorin, V.V., Kukushkin, Y.S., van der Loo, J.C.M., and Johnstone, E.C. (2021). The clinical landscape for AAV gene therapies. Nat. Rev. Drug Discov. *20*, 173–174. https://doi.org/10.1038/d41573-021-00017-7.

49. Tran, N.T., Danner, E., Li, X., Graf, R., Lebedin, M., de la Rosa, K., Kühn, R., Rajewsky, K., and Chu, V.T. (2022). Precise CRISPR-Cas–mediated gene repair with minimal off-target and unintended on-target mutations in human hematopoietic stem cells. Sci. Adv. *8*, eabm9106. https://doi.org/10.1126/sciadv.abm9106.

50. Andersen, S., Wolff, J.H., Skov, T.W., Janns, J.H., Davis, L.J., Haldrup, J.H., Haslund, D., Revenfeld, A.L., Relkovic, D., Møller, B.K., et al. (2025). Gene editing in hematopoietic stem cells by co-delivery of Cas9/sgRNA ribonucleoprotein and templates for homology-directed repair in 'all-in-one' lentivirus-derived nanoparticles. Nucleic Acids Res. *53*, gkaf767. https://doi.org/10.1093/nar/gkaf767.

51. Geilenkeuser, J., Armbrust, N., Steinmaßl, E., Du, S.W., Schmidt, S., Binder, E.M.H., Li, Y., Warsing, N.W., Wendel, S.V., von der Linde, F., et al. (2025). Engineered nucleocytosolic vehicles for loading of programmable editors. Cell *188*, 2637–2655.e31. https://doi.org/10.1016/j.cell.2025.03.015.

52. Jo, D.-H., Kaczmarek, S., Shin, O., Wang, L., Cowan, J., McComb, S., and Lee, S.-H. (2023). Simultaneous engineering of natural killer cells for CAR transgenesis and CRISPR-Cas9 knockout using retroviral particles. Mol. Ther. Methods Clin. Dev. *29*, 173–184. https://doi.org/10.1016/j.omtm.2023.03.006.

53. Suchy, F.P., Karigane, D., Nakauchi, Y., Higuchi, M., Zhang, J., Pekrun, K., Hsu, I., Fan, A.C., Nishimura, T., Charlesworth, C.T., et al. (2025). Genome engineering with Cas9 and AAV repair templates generates frequent concatemeric insertions of viral vectors. Nat. Biotechnol. *43*, 204–213. https://doi.org/10.1038/s41587-024-02171-w.

54. Magnus, J., and Käsbach, J. (2025). A clinician's guide to AAV production - How manufacturing platforms shape vector properties. Med. Genet. *37*, 169–177. https://doi.org/10.1515/medgen-2025-2024.

55. Sripada, S.A., Hosseini, M., Ramesh, S., Wang, J., Ritola, K., Menegatti, S., and Daniele, M.A. (2024). Advances and opportunities in process analytical technologies for viral vector manufacturing. Biotechnol. Adv. *74*, 108391. https://doi.org/10.1016/j.biotechadv.2024.108391.

56. Mazarakis, N.D., Azzouz, M., Rohll, J.B., Ellard, F.M., Wilkes, F.J., Olsen, A.L., Carter, E.E., Barber, R.D., Baban, D.F., Kingsman, S.M., et al. (2001). Rabies virus glycoprotein pseudotyping of lentiviral vectors enables retrograde axonal transport and access to the nervous system after peripheral delivery. Hum. Mol. Genet. *10*, 2109–2121. https://doi.org/10.1093/hmg/10.19.2109.

57. Mirow, M., Schwarze, L.I., Fehse, B., and Riecken, K. (2021). Efficient Pseudotyping of Different Retroviral Vectors Using a Novel, Codon-Optimized Gene for Chimeric GALV Envelope. Viruses *13*, 1471. https://doi.org/10.3390/v13081471.

58. Andorko, J.I., Russell, R.M., Schnepp, B.C., Grubaugh, D., Mullen, K.F., Wakabayashi, A., Carrington, L.J., O'Malley, T., Kuri-Cervantes, L., Culp, T.D., and Johnson, P.R. (2025). Targeted in vivo delivery of genetic medicines utilizing an engineered lentiviral vector platform results in CAR T and NK cell generation. Mol. Ther. *33*, 4937–4952. https://doi.org/10.1016/j.ymthe.2025.06.036.

59. Frank, A.M., Braun, A.H., Scheib, L., Agarwal, S., Schneider, I.C., Fusil, F., Perian, S., Sahin, U., Thalheimer, F.B., Verhoeyen, E., and Buchholz, C.J. (2020). Combining

T-cell–specific activation and in vivo gene delivery through CD3-targeted lentiviral vectors. Blood Adv. *4*, 5702–5715. https://doi.org/10.1182/bloodadvances.2020002229.

60. Michels, K.R., Sheih, A., Hernandez, S.A., Brandes, A.H., Parrilla, D., Irwin, B., Perez, A.M., Ting, H.-A., Nicolai, C.J., Gervascio, T., et al. (2023). Preclinical proof of concept for VivoVec, a lentiviral-based platform for in vivo CAR T-cell engineering. J. Immunother. Cancer *11*, e006292. https://doi.org/10.1136/jitc-2022-006292.

61. Raguram, A., An, M., Chen, P.Z., and Liu, D.R. (2025). Directed evolution of engineered virus-like particles with improved production and transduction efficiencies. Nat. Biotechnol. *43*, 1635–1647. https://doi.org/10.1038/s41587-024-02467-x.

62. Hamilton, J.R., Chen, E., Perez, B.S., Sandoval Espinoza, C.R., Kang, M.H., Trinidad, M., Ngo, W., and Doudna, J.A. (2024). In vivo human T cell engineering with enveloped delivery vehicles. Nat. Biotechnol. *42*, 1684–1692. https://doi.org/10.1038/s41587-023-02085-z.